Characterization of Pilot Technique

Edward Bachelder
Senior Research Engineer
San Jose State University,
US Army Aviation
Development Directorate
Moffett Field, CA, USA

Bimal Aponso
Branch Chief,
Aviation Systems Division
NASA Ames Research Center
Moffett Field, CA, USA

Martine Godfroy
Senior Research Scientist
San Jose State University,
NASA Ames Research Center
Moffett Field, CA, USA

ABSTRACT

Skilled pilots often use pulse control when controlling higher order (i.e. acceleration-command) vehicle dynamics. Pulsing does not produce a stick response that resembles what the human Crossover Model (Ref.1) predicts. The Crossover Model (CM) assumes the pilot provides compensation necessary (lead or lag) such that the suite of display-human-vehicle approximates an integrator in the region of crossover frequency. However, it is shown that the CM does appear to drive the pilots' pulsing behavior in a very predictable manner. Roughly speaking, the pilot generates pulses such that the area under the pulse (pulse amplitude multiplied by pulse width) is approximately equal to area under the hypothetical CM output. This can allow a pilot to employ constant amplitude pulsing so that only the pulse duration (width) is modulated – a drastic simplification over the demands of continuous tracking. A pilot pulse model is developed, with which the parameters of the pilot's internally-generated CM can be computed in real time for pilot monitoring and display compensation. It is also demonstrated that pursuit tracking may be activated when pulse control is employed.

NOTATION

Y_p	=	pilot describing function
Y_c	=	controlled element transfer function
τ	=	pilot time delay
K	=	pilot gain
z	=	pilot lead frequency
δ	=	pilot control input
e	=	displayed error
CM	=	Crossover Model
TF	=	Transfer Function

INTRODUCTION

In a single-axis tracking experiment conducted by Bachelder (Ref. 2) which investigated the relationship between pilot response and pilot workload, it was observed that pilots employing pulse control consistently outperformed pilots employing continuous tracking (when using acceleration or jerk-command vehicle dynamics). There are two significant mathematical properties associated with the pulse: 1) within the width of the pulse the control input is a step, during which the vehicle dynamics being controlled are integrated in time. Any other control input (ramp, sine, etc.) would result in a more complex response; 2) when the pulse ceases, the response is fundamentally an integration of the derivative of the vehicle dynamics, which means the order of the original dynamics is reduced by one. Thus a pulse input produces the most simple vehicle response possible both during the pulse, and after the pulse. It is hypothesized this could allow a skilled pilot to mentally decouple the aircraft motion due to control input from the motion arising from atmospheric disturbance. Such a condition could enable pursuit tracking (where the effect of the disturbance on the target state is observed as distinct from the effect of pilot input on the target state), which has been shown in research to improve performance over purely compensatory tracking (where the effects of disturbance and input are combined and presented as one error). When pursuit tracking is added to the Pulse Model, the pulse actuation predicted by the model matched observed pilot response even better than when just compensatory tracking was assumed. This hypothesized behavior will be verified using additional pilot data, and if correct it will represent a significant contribution to manual control theory, in addition to offering a basis for including pulse control in pilot instruction.

If the aircraft dynamics being controlled are uncertain or highly nonlinear, it is not possible to estimate with precision the effective pilot parameters (gain, time delay, lead, lag). Furthermore, even if the effective parameters can be established, if the pilot control strategy contains nonlinearities (i.e. strategies such as amplitude clipping or pulsing), the difference between effective and actual pilot parameters can be significant. To give a practical example of how this can be important, Ref. 3 showed that pilot stick activity can be used to compute pilot cutoff frequency, which provides an estimate of task bandwidth. However, this technique becomes less precise as pilot nonlinearity increases. Precision is regained if the output of the underlying CM (which is computed by the proposed Pilot Pulse Model) is employed instead of the raw stick data.

Presented at the AHS International 73rd Annual Forum & Technology Display, Fort Worth, Texas, USA, May 9-11, 2017.

Pulsing also allows a pilot maximum time to scan the environment (out-the-window scene, cockpit instruments) without sacrificing performance, which is not possible if continuous tracking were employed.

It is also shown that control strategy can have an effect on pilot workload estimation, thus modeling a pilot's control output is important for predicting his/her control parameters and associated workload for a given task. Different pulsing strategies are modeled, and comparisons between various pilot control strategies (continuous, amplitude clipping, pulsing) in the presence of pilot noise are given.

EXPERIMENTAL PROTOCOL

Various command vehicle dynamics (proportional, rate, acceleration, jerk), vehicle gains (vehicle sensitivity to input), and display gains (display sensitivity to error) were used with a lateral station-keeping using a compensatory display, where a random forcing function continuously disturbed ownship's position.

Figure 1a shows a schematic of the station-keeping task and the display, pilot and vehicle components of the closed-loop system. Figure 1b gives the range of conditions within each component that were tested. The jerk condition for the vehicle dynamics (fourth condition listed for YV), contains a pole p whose location was varied. Twenty-three display configurations were tested with each subject using various combinations of the conditions shown in Figure 1b. Since pilot proficiency with any test condition was not a factor in this experiment, pilots were given two practice of each vehicle dynamic type (proportional, rate, acceleration, jerk) prior to testing.

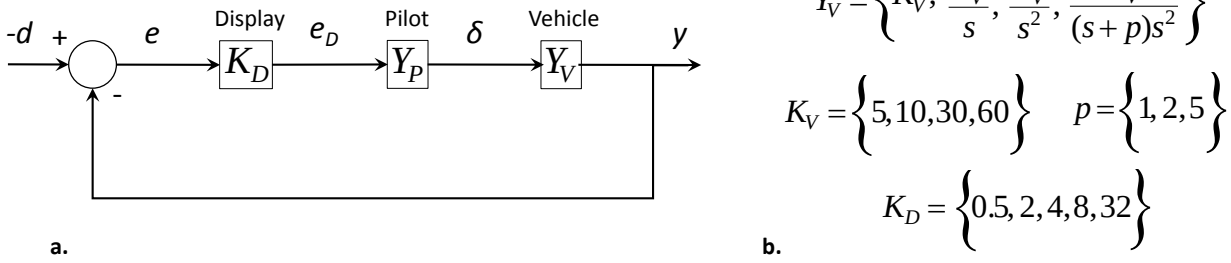

$$Y_V = \left\{ K_V,\ \frac{K_V}{s},\ \frac{K_V}{s^2},\ \frac{K_V}{(s+p)s^2} \right\}$$

$$K_V = \{5, 10, 30, 60\} \qquad p = \{1, 2, 5\}$$

$$K_D = \{0.5, 2, 4, 8, 32\}$$

b.

Figure 1. Station-keeping task. ***a) Pilot, display, and vehicle elements; b) Range of conditions for display and vehicle elements.***

One may be tempted to think that the display gain and the vehicle gain are effectively interchangeable and the same gains from the pilot's vantage point. The following example will serve to disprove this common misnomer. If the pilot's input is zero, the disturbance is perceived through the display gain – the vehicle gain does not come into play at all. Based on his/her control activity and quiescence, a pilot learns to decouple the effects of the display gain from the vehicle gain – thus decoupling aircraft motion due to disturbance from pilot-commanded vehicle motion.

The components of the pilot element Yp of Figure 1 are shown in Figure 2. Pilot visual noise is added to the displayed error (Ref. 1), the sum is operated on by the Crossover Model (CM, Ref. 1) pilot. The output of this is then sent through a limiter.

Four male participants took part in the study. Three were Experimental Test Pilots (graduates of Navy Test Pilot School) with 1,900, 1,900, and 2,450 rotary wing flight hours. The fourth participant had logged 800 hours of rotary wing flight time. Ownship error relative to the hover location was displayed on a laptop monitor (see Figure 3), and the pilot attempted to minimize the error using a gaming joystick. The Bedford rating scale (Ref.4) was used to subjectively score each pilots spare capacity at the end of each 60-second tracking run. Dependent variables were: stick position, rate and acceleration, stick position reversals, display error, rate, and acceleration. The positional disturbances imposed on the helicopter were designed to be both realistic and a diagnostic probe for pilot control behavior. Composed of a sum of 11 non-harmonically-related sine waves, the disturbance was perceived by the pilot as a random process – the result, however, was that the pilot's control response power resided largely at the same frequencies contained in the input disturbances. The disturbance time history is shown in Figure 3.

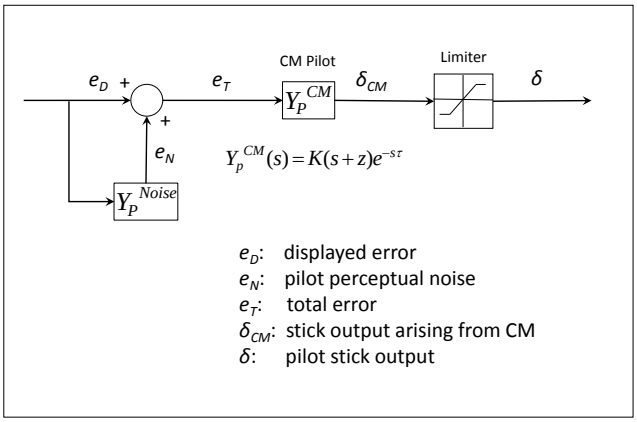

Figure 2. Components of Pilot element Y_p shown in Figure 2a.

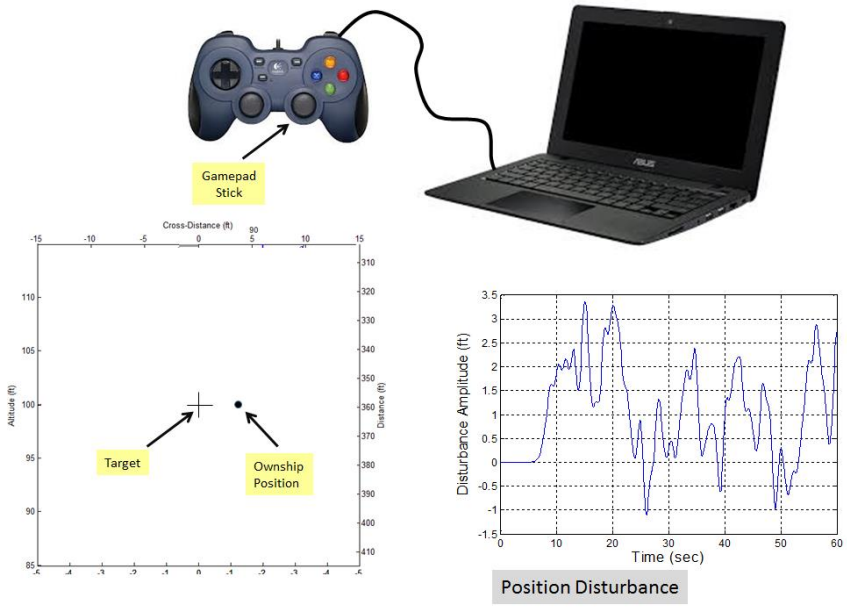

Figure 3. Simulation environment.

WORKLOAD ANALYSIS

In this station-keeping experiment the variables that correlated best with subjective rating were stick rate and display error rate. The two variables were combined in an empirically-derived relationship and to produce Bedford estimates of the 92 data points shown in Figure 5a (coefficient of determination is 0.91). Figure 5b gives the operations conducted on stick position and display error to produce the Bedford estimate.

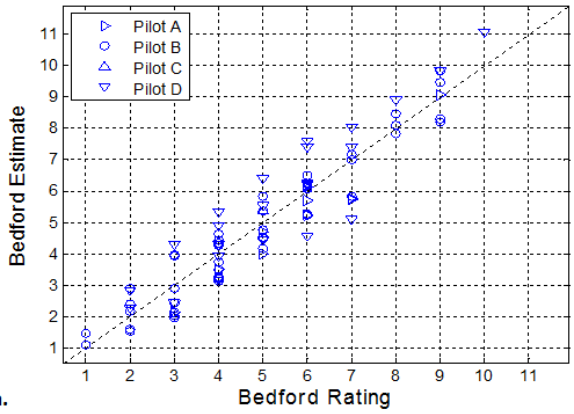

a.

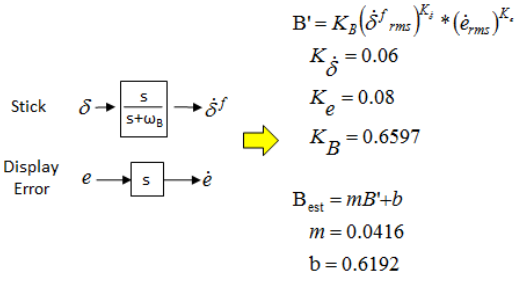

b.

Figure 5. Bedford Estimate: a) Results (coefficient of determination 0.90); b) Computation of Bedford Estimate.

The Bedford rating scale is based on descriptors and a decision tree similar to what the Cooper-Harper HQR uses, and likewise is ordinal. The Bedford rating scale allows the ordering of workload from insignificant (1) to uncontrollable (10). It would be desirable if the rating was interval, allowing differences to be measured as a continuum. In Ref. 5 Mitchell and Aponso demonstrated that the use of the ordinal Cooper-Harper HQRs as if they were interval was both reasonable. Given the similarities between the Bedford and Cooper-Harper ratings, it is assumed that the same argument for treating the Bedford rating as interval can be made.

To test reasonableness of the Bedford estimator it was applied to helicopter multi-axis flight. Seventy-nine helicopter instrument approaches – in actual degraded visual environment (DVE) flight - were executed by five Army evaluation pilots using a head-down display to track a commanded approach profile. The display used (Integrated Cueing Environment display, an Army developmental cueing set) is shown in Figure 4. Upon completion of an approach the pilot provided a Bedford rating. In Figure 5a each control axis (lateral cyclic, longitudinal cyclic, collective, pedals) is normalized by the largest displacement encountered in all the data. Lateral and longitudinal cyclic motion were combined since the display presented error to the pilot as a single distance and direction. Display error was converted to degrees as viewed from the pilot's distance. The Bedford estimate for each control axis (cyclic, collective, pedals) was computed over a sliding window of eight seconds using the relationships between control rate and display error rate given in Figure 5b, and the maximum of the three estimates at every time increment was used to create the combined history shown in Figure 6a. The mean of the entire flight segment of interest gives the estimate of the overall rating for the segment. Figure 6a gives the distribution of ratings (% of total collected), and 6b plots the mean and standard deviation bars of data overlaid on the line representing ideal correspondence between the estimated and actual pilot rating.

Given that the Bedford estimator was developed from a single-axis simulation task experiment, and that the DVE flight test conditions presented the pilots with multi-modal cueing (tactile, audio) and a mixed visual environment (head-down display and a distracting out-the-window scene of actual blowing dust), these preliminary results are encouraging. It appears the proposed Bedford estimator appears to be effective for this complex task in the UH-60.

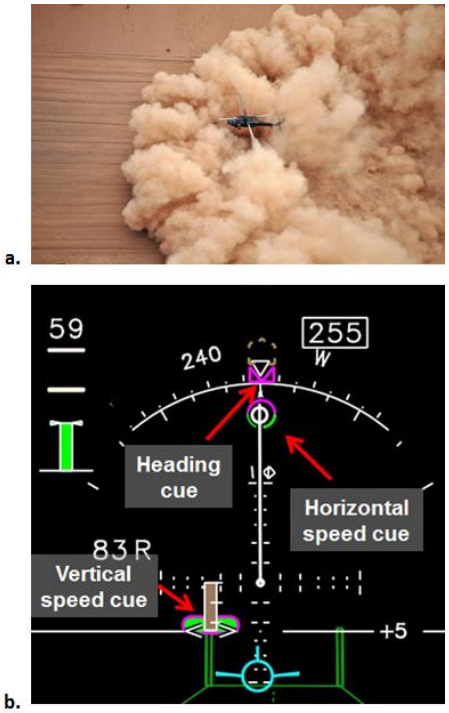

Figure 4. a) DVE operations; b) Integrated Cueing Environment (ICE) display.

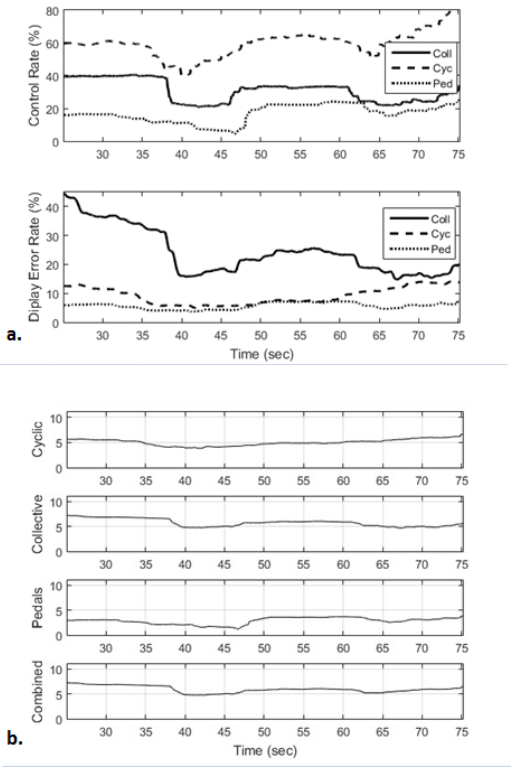

Figure 5. Application of Bedford estimator to multi-axis helicopter flight. a) Control and display error rates; b) Time history of Bedford estimates for cyclic, collective, pedals, and aggregate.

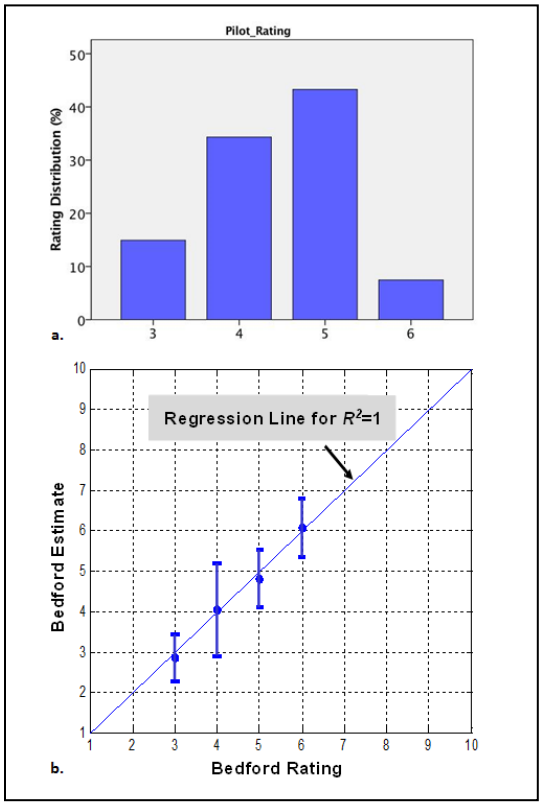

Figure 6. Bedford estimator: **a) Distribution of ratings collected (%, sample size was 79 flights);** b) **Bedford estimator flight test results.**

PILOT TECHNIQUE

Large differences can arise between the response predicted by McRuer's *CM* and actual pilot data, especially when the vehicle being controlled has dynamics that require significant lead compensation by the pilot. Figure 7 shows stick responses for three different pilots conducting the same station-keeping task and same condition (acceleration-command vehicle dynamics, identical stick and display gain) in the simulation experiment described above. Three different control techniques are evident from close-ups of the histories shown in Figure 8: a) Amplitude clipping, where stick response is continuous except for limiting occurring at approximately 50% of full stick throw; b) Pulse width modulation, where full stick throw is employed and only the width of the pulse is varied; c) Pulse width and pulse amplitude modulation. Each pilot was consistent in technique when using the same vehicle dynamics for other conditions (display and stick gains). Pulse control and amplitude clipping models are developed in the following sections.

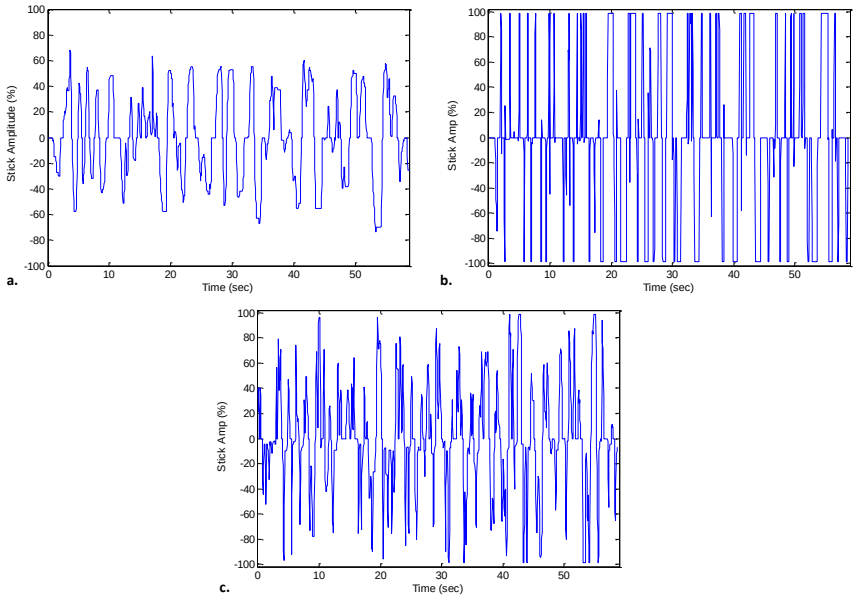

Figure 7. Stick time histories for three different pilots (same station-keeping task, acceleration-command vehicle dynamics): a) Amplitude clipping; b) Pulse width modulation; c) Pulse width-amplitude modulation.

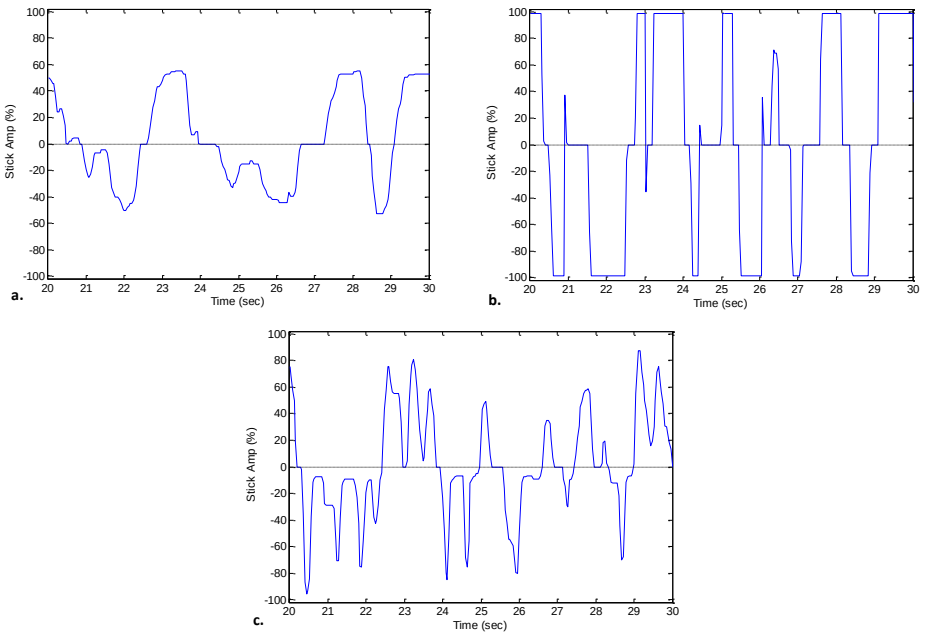

Figure 8. Close-up of stick time histories shown in Figure 7: a) Amplitude clipping; b) Pulse width modulation; c) Pulse width-amplitude modulation.

Amplitude Clipping

A nonlinear pilot control technique, observed and coined by the authors as 'amplitude clipping', occurs when a pilot limits his/her control input to some fixed amplitude over a short period of time rather than responding continuously to the error signal. Thus the pilot responds to an error similar to what the *CM* predicts up to a certain stick amplitude that remains fixed until the error signal reverses and returns, at which time the pilot resumes active tracking. The amplitude at which the control input is capped can vary over time.

Amplitude clipping lowers the effective gain of the pilot, as it is the equivalent of saturation. Ref. 6 graphs the gain attenuation for a sinusoid of amplitude ***A*** that saturates at amplitude ***a***, shown in Figure 9.

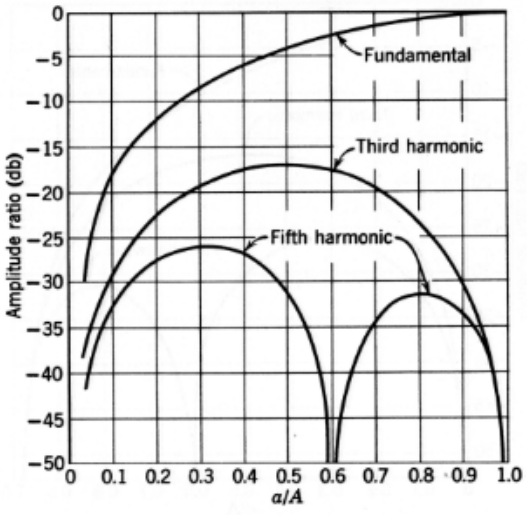

Figure 9. Sinusoidal describing function for saturation (Ref. 6).

The actual pilot stick response in Figure 10 shows that the pilot limits (clips) the input at approximately 50% of maximum displacement. Figure 11a compares the same pilot actual stick response to a simulated pilot stick response generated by the pilot model, and clips this simulated stick signal using the actual pilot's stick min/max segments as a template. The pilot parameters associated with the *CM* (time delay, gain, and lead) used in the pilot model are given in Eq. (1).

$$Y_P(s) = K(s+z)e^{-s\tau} \tag{1}$$

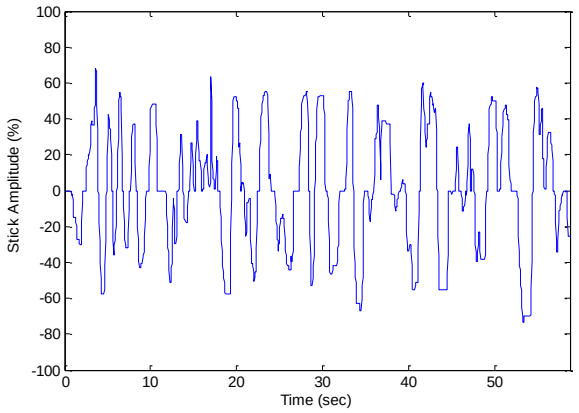

Figure 10. Pilot stick data from station-keeping task.

Figure 11 defines clipping area as the portion of the *CM* stick output that is clipped relative to the total *CM* stick output. Figure 12 presents time histories of the computed Bedford estimate and percentage clipping area for a low and a high workload run. It appears that the workload slightly dips when clipping increases, and increases when clipping is reduced. When a pilot employed clipping, mean clipping area was observed to correlate with the overall workload rating. McRuer had noted that a rise in pilot lead generation was accompanied by an increase in pilot perceptual 'noise' that was uncorrelated with the error, which he called 'control remnant'. The preliminary data from this experiment indicates that part of this remnant can be due to performance-enhancing nonlinear pilot techniques such amplitude-clipping and pulsing. Other potential source of remnant during flight operation would be divided attention (i.e. scanning).

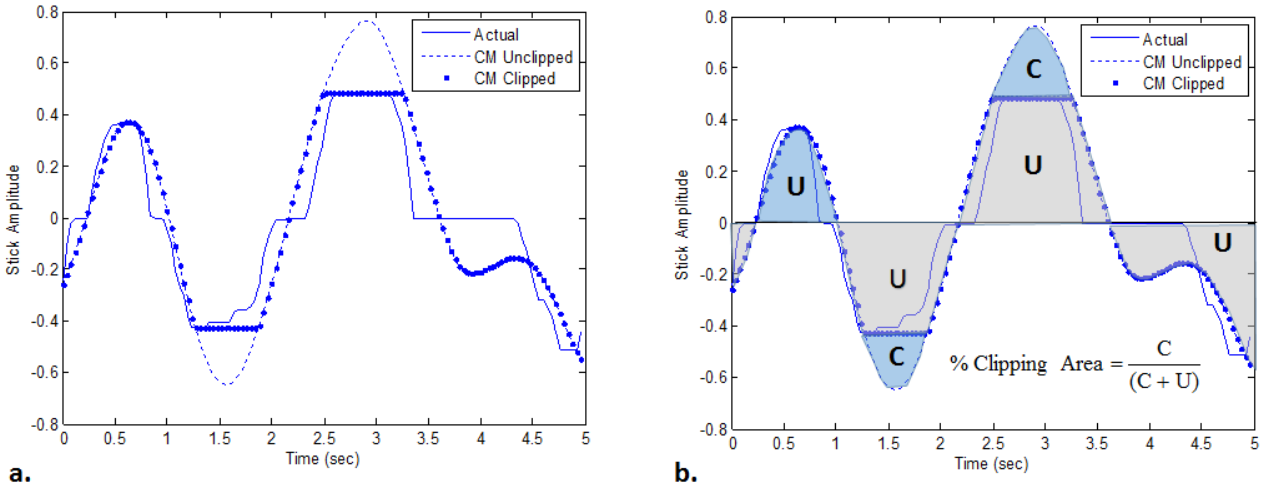

Figure 11. a) Comparison of actual stick data, unclipped Crossover Model (CM) response, and clipped CM response; b) % clipping area defined.

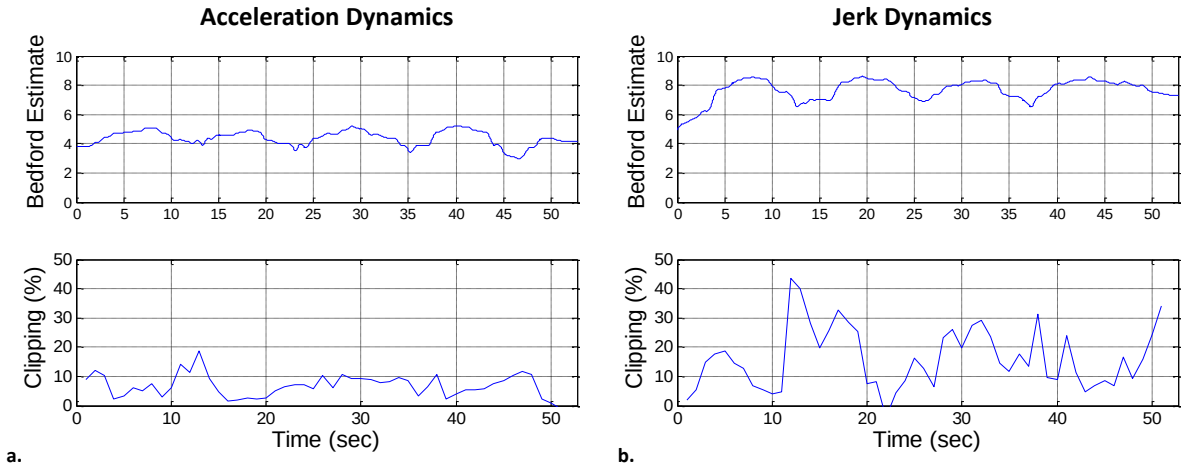

Figure 12. Bedford estimate and clipping area time histories. a) Acceleration dynamics (overall Bedford rating 4); b) Jerk dynamics (high workload, overall Bedford rating 8).

Using the clipped simulated pilot response (see Fig. 11), the three parameters of the pilot model (Fig. 2) are iteratively varied and filtered until a best match is computed between the actual and simulated/clipped stick. This parameter identification is conducted over a sliding time window, allowing near real-time measurement. In Figure 13 the values of the pilot parameters used in a simulation of the pilot were fixed (denoted as truth by dash-dot lines) over the course of the run. The solid line shows the identification when clipping is accounted for, and the dashed line denotes the identification when clipping is not taken into account. In all three cases accounting for clipping produced very good matching with the actual parameters. In Figure 13a, the non-clipped gain falls to almost 50% of the true CM gain – this represents the effective reduction in open-loop gain due to clipping. Non-clipped time delay has a transient excursion from truth, and non-clipped lead rises to twice the actual value before decreasing. Thus if clipping is not considered, the values computed can be misleading as to what is actually occurring in the pilot.

To test the method's efficacy during dynamic pilot changes, parameters of an actual pilot were identified over time. These parameter time histories drove the pilot simulation that was used in Figure 13, and in turn the parameters identified from the simulation were compared with the parameters originally obtained from the pilot data. After shifting the observed histories in time by half of the sliding time window that was used (the window was eight seconds, the average lag would be half of this), Figure 14 shows near-perfect correspondence between the original and recovered pilot values.

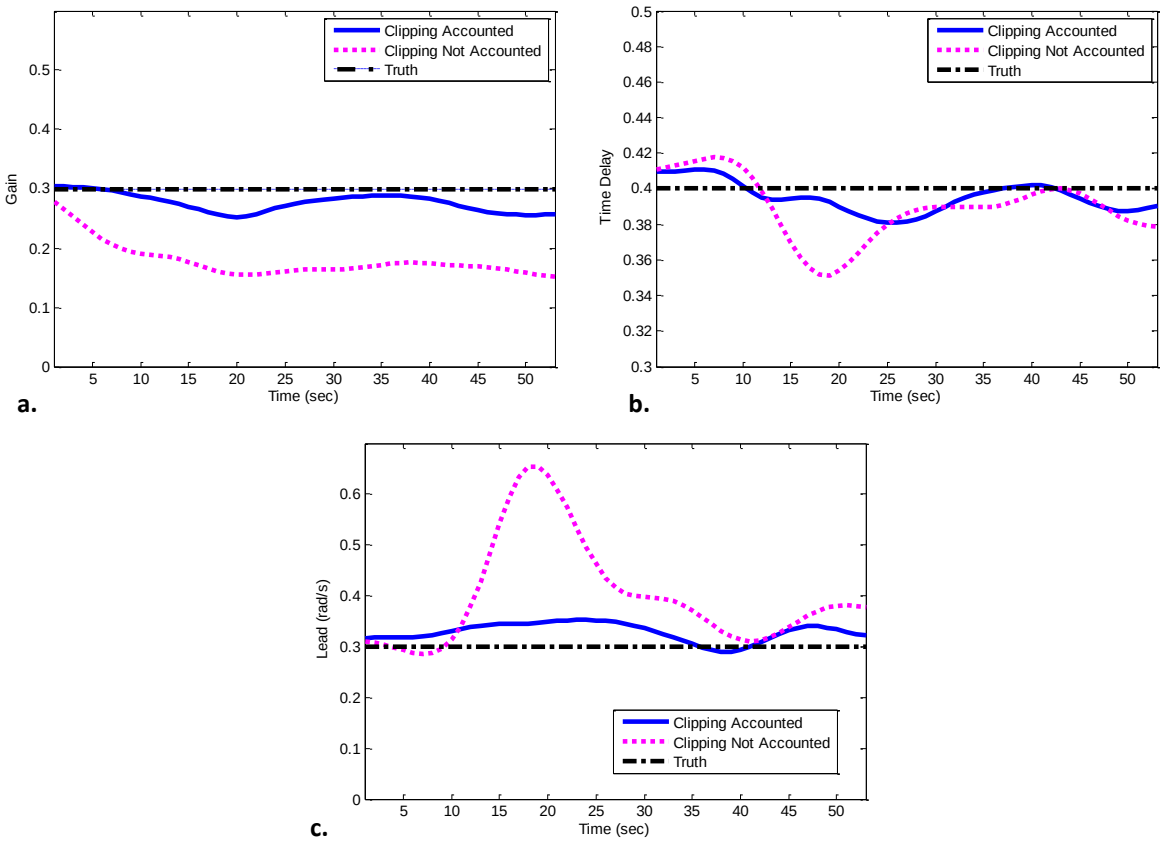

Figure 13. Effect of accounting/not accounting for clipping on pilot parameter identification. a) Pilot gain; b) Pilot time delay; c) Pilot lead frequency.

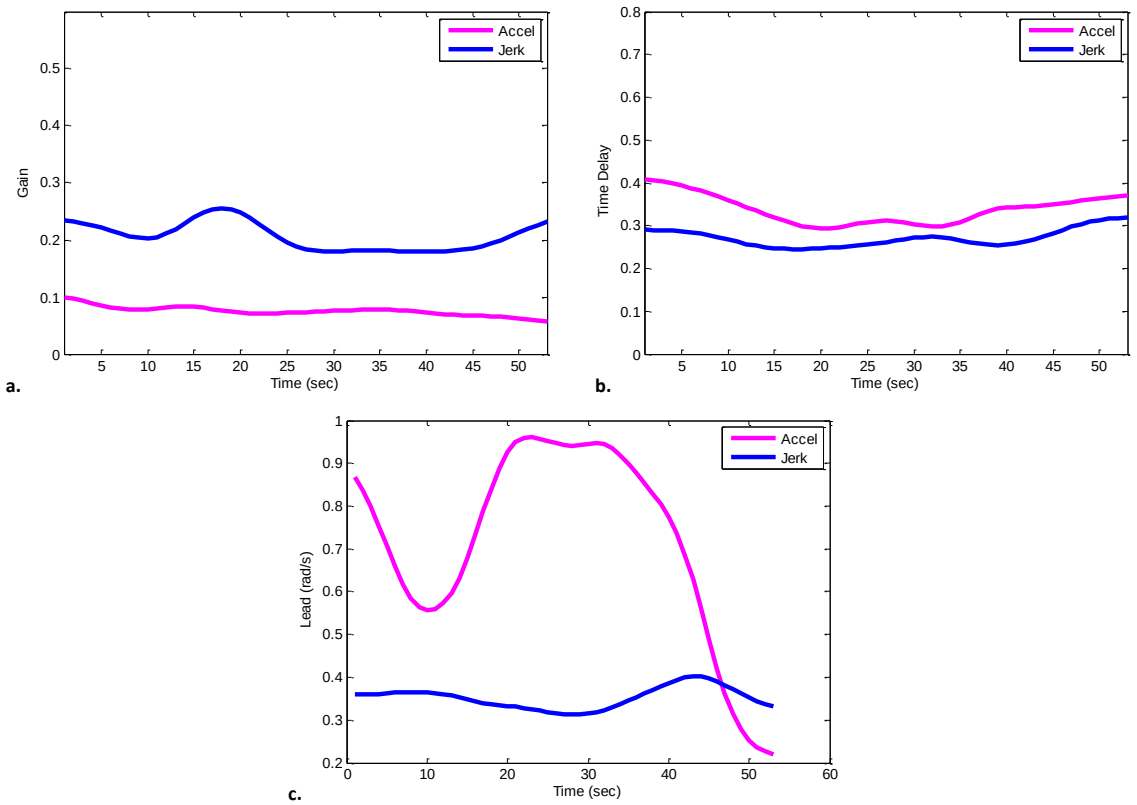

Figure 14. Pilot parameters identified and cross-checked. ***a) Pilot gain; b) Pilot time delay; c) Pilot lead frequency.***

The effects of pilot technique and changes in pilot parameters are now examined using the pilot model. In Table 1 performance (RMS error) is roughly the same comparing 50% clipping and no clipping for the nominal pilot parameters (0.4 second time delay, gain of 0.2). Clipping, however, yields a somewhat lower Bedford estimate. Doubling the pilot gain to 0.4 (pilot tracks more aggressively) slightly increases the RMS error for both techniques due to the time delay, however workload substantially increases for the no clipping case (workload only moderately rises when clipping is employed). Increasing pilot time delay from 0.4 seconds to 0.9 seconds produces a substantial rise in error and workload from the nominal when clipping is not used, whereas the performance degradation is less when clipping is used, and results in almost no increase in workload (for the no clipping case, stick output is limited to 100% when it reaches the limit of throw). It is worth repeating that clipping consistently produced a lower Bedford rating. While a pilot would not be expected to persist in maintaining parameters that give poor performance, these examples serve to show how amplitude clipping would allow a system to absorb transient excursions in pilot parameters and permit continued satisfactory performance.

Table 1. Comparison of RMS error and Bedford estimates with and without clipping.

Time Delay (sec)	Gain	Clipping	RMS Error (ft)	Bedford Est
0.4	0.2	no	0.9	6.5
0.4	0.2	50%	1.0	6.1
0.4	0.4	no	1.2	8.0
0.4	0.4	50%	1.3	6.7
0.9	0.2	no	2.2	7.7
0.9	0.2	50%	1.6	6.4

The pilot model shown earlier in Figure 2 was used with and without the presence of pilot perceptual noise, and subjective ratings using the Bedford estimator were generated. Figure 15 shows the % increase in RMS error and associated % decrease in Bedford rating (referred to as an elasticity analysis in Economics) for both amplitude clipping and continuous tracking. The curve for each technique started with the same point (same gain, no clipping), yielding an initial RMS error and Bedford estimate. To generate the clipping curve, clipping was progressively increased with gain held constant, and the percent changes in RMS error and Bedford estimate relative to the starting values produced the ordinate and abscissa pairs. To generate the continuous tracking gain adjustment curve, gain was decreased (no

clipping used). Figure 15a indicates that when perceptual noise is absent, then for the same decrement of performance the task would be easier using the continuous tracking gain reduction compared to when clipping reduces gain. However, with the addition of perceptual noise, Figure 15b shows that amplitude clipping can generate a faster decrease in workload than continuous tracking for the same increase in RMS tracking error. For this example, clipping amplitude at 50% of full stick motion results in less workload than if continuous tracking were used to generate the same RMS error (that 50% amplitude clipping produces). Another important advantage clipping offers is the opportunity for the pilot to scan other visual cues or events in the environment while the clipping is occurring. Furthermore, it appears that clipping enhances system robustness to transient changes in pilot time delay and CM gain, which could allow more relaxed operation.

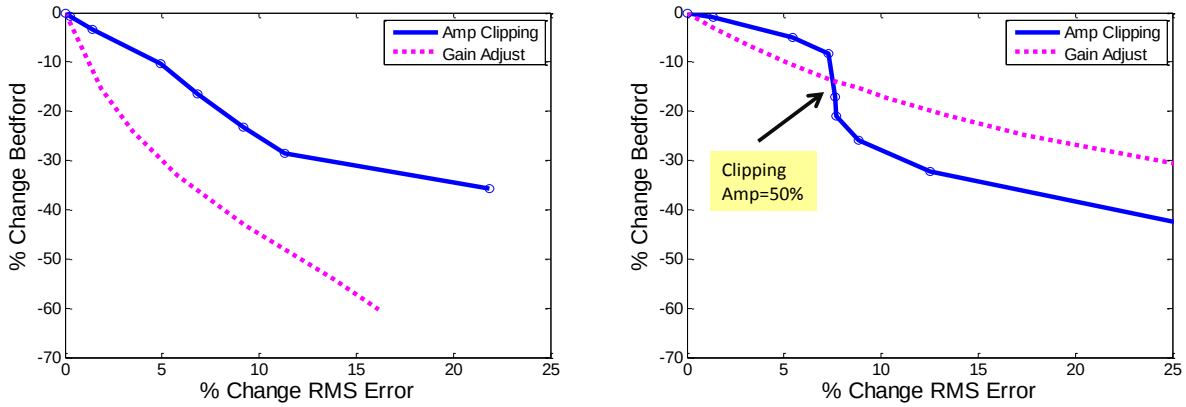

Figure 15. Elasticities using amplitude clipping and continuous tracking gain adjustment (acceleration dynamics). a) Without pilot perceptual noise; b) With pilot perceptual noise.

Pulse Control

The frequency response of the open-loop system y/e (Figure 16) for the pulse width modulation control example used in Figure 7 was computed at the frequencies of the sum-of-sines using power spectral density (psd) ratios of the display input (aircraft positional error) and the aircraft position response due to pilot control. The system identification tool CIFER® (Comprehensive Identification from FrEquency Responses) was used to generate the frequency response, represented by the ovals in Figure 17. Parameters of the CM were then iterated to yield a best match with the measured frequency response, represented by the smooth line in Figure 17. Note a low-frequency phase loss parameter, as described in Ref. 1, is used in the model.

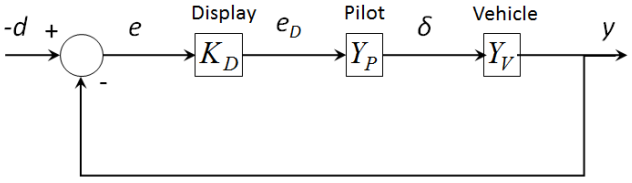

Figure 16. Elements of station-keeping task.

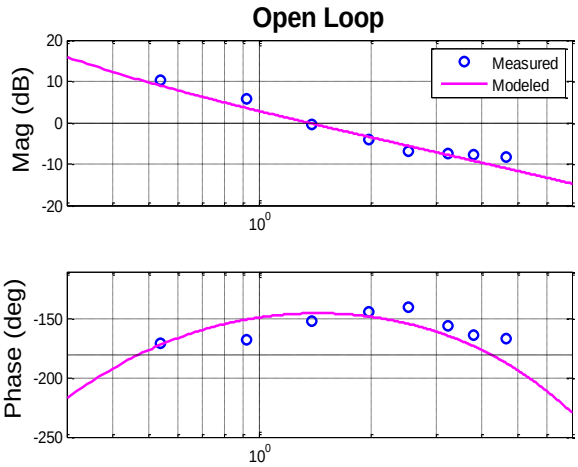

Figure 17. Measured frequency response of open-loop using pilot data (pulse-control) and CM responses.

The CM using the best-fit parameters of Figure 17 was employed to generate a simulated pilot response using the actual tracking error history of the of the pilot's data run. This is overlaid on the pilot's actual stick response in Figure 18. There appears to be a pulse associated with each zero crossing of the CM output, as well as a pulse occurring with each speed reversal of the CM. However, the duration (width) of each pulse and the occurrence of additional pulses between zero crossings is not apparent.

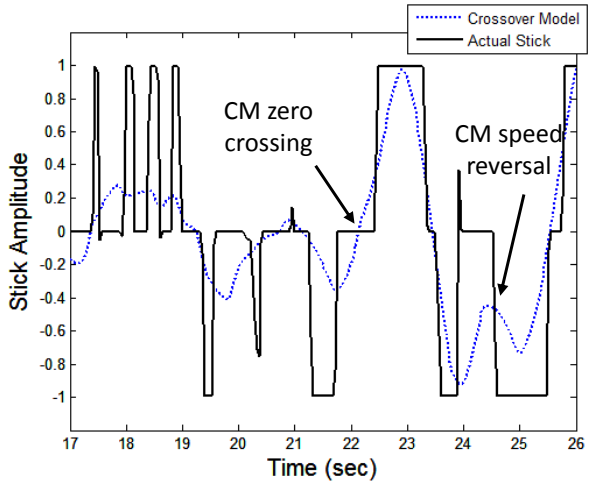

Figure 18. Actual stick response overlaid on CM output.

It was hypothesized that the pilot uses the cumulative area under the CM between zero crossings to modulate pulses. Figure 19 plots the cumulative areas under the CM and actual stick that accrue between the CM zero crossings. In general the two appear to progress synchronously.

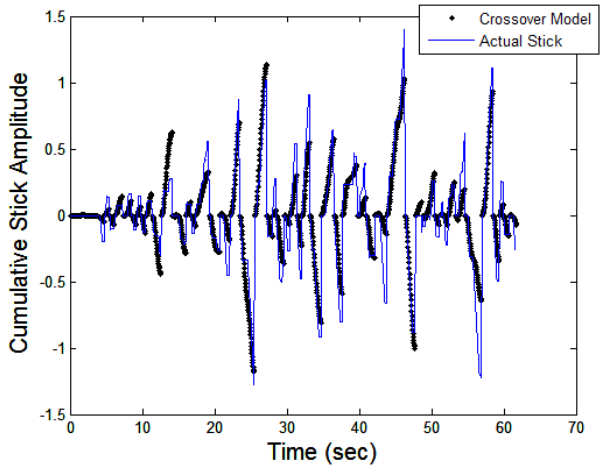

Figure 19. Comparison of cumulative area under the Crossover Model and actual pilot stick (between CM zero crossings).

Only past information on the CM response (up to the current moment in time) would be available to the pilot for governing his/her pulse response. Thus it was assumed that pulses are triggered based on cumulative CM area events. The following set of rules were created to test this assumption.

If Zero_Crossing or Speed_Reversal
Fire = 1

If $Cum\_Area_{Pulse} > F_1 * Cum\_Area_{CM}$
Fire = 0

If $Cum\_Area_{Pulse} < F_2 * Cum\_Area_{CM}$
Fire = 1

Figure 20. Rules linking cumulative CM and pulse areas to pulse response.

Figure 21 compares the outputs of the CM, actual stick, and pulse model. Figure 22 compares the stick power spectral densities of the actual pilot and pulse model. Given the stochastic nature of the pilot timing pulses with an internally integrated model, agreement in both figures between actual stick and modeled responses is good.

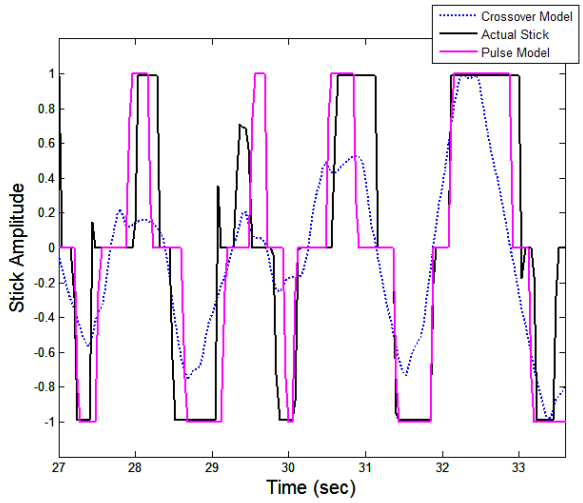

Figure 21. Comparison of the Crossover Model, actual pilot stick, and pulse model outputs.

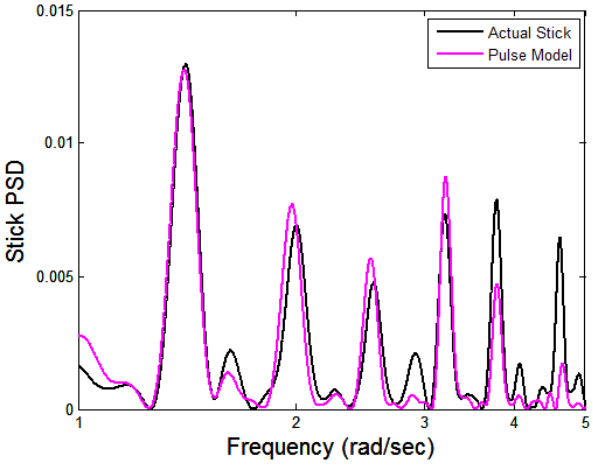

Figure 22. Power spectral density comparison of the actual pilot stick and pulse model outputs.

Pursuit and Pulse Control

It is hypothesized pulsing could allow a skilled pilot to mentally decouple the aircraft motion due to control input from the motion arising from atmospheric disturbance. Such a condition could enable pursuit tracking (where the effect of the disturbance on the target state is observed as distinct from the effect of pilot input on the target state), which has been shown in research to improve performance over purely compensatory tracking (where the effects of disturbance and input are combined and presented as one error). In his

watershed work on human pilot behavior (Ref. 1), McRuer proposed the Dual Channel model to represent how an operator blends a) information of the reference (in station-keeping this is the disturbance) signal being tracked with b) error between the reference and the system output. Figure 23 shows the McRuer Dual Channel model modified to let a fraction f_d of the feedforward from *d* pass into the loop. The relationship between pilot stick and received error is given by Equation 3 below. When f_d is unity, the error is driven to zero when the feedforward pilot element Y_d becomes the inverse of the vehicle dynamics. However, Y_d would be subject to the same pilot time delay as the compensatory element acting on the error Y_e (Y_e is the CM), so that Y_d would assume the form given in Eq. 2.

$$\frac{\delta}{e} = \frac{f_d Y_d + Y_e}{1 - f_d Y_d Y_v}, \quad Y_d \approx \frac{e^{-\tau s}}{Y_v} \tag{2}$$

It was observed that the match between the pulse model and actual stick spectral response (Figure 22) improved when pursuit tracking was added to the CM's compensatory tracking using $f_d = 0.15$. Furthermore, the match between the modeled and measured frequency response (notably in phase) improved. The data of the other pilot who exhibited pulse control (Figure 7c) was examined for a similar trend. The same pulse model used for this analysis, except a fixed amplitude of 0.6 was used to represent an average of the modulated amplitude that the pilot produced. The results were even more marked than with the previous pilot. Figure 24a and b compare the effect of pursuit tracking on the stick spectral response, where the addition of pursuit (once again using the feedforward fraction $f_d = 0.15$) produces a near-perfect match between model and actual. Using the same pilot time delay to generate the frequency responses of Figure 24c and d, it is seen that the addition of pursuit yields an excellent fit for phase, whereas its absence produced a poor phase fit.

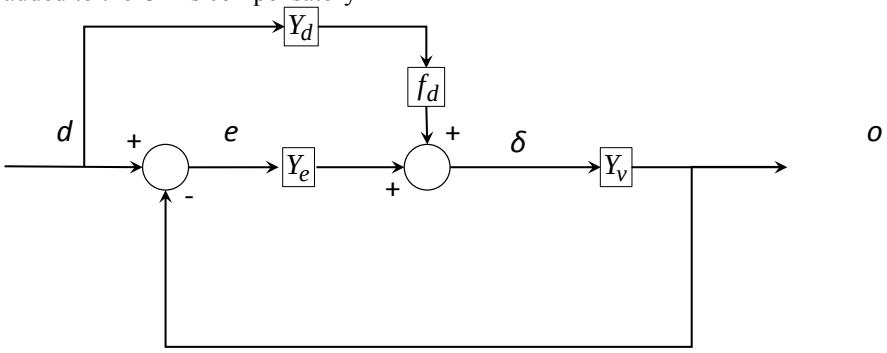

r: reference
e: error
δ: control input
d: disturbance
o: system output

TF: transfer function
Y_d*: pilot TF, disturbance component*
Y_e*: pilot TF, error component*
Y_v*: vehicle element*
f_d*: fraction of disturbance path passed through*

Figure 23. Dual Channel model (Ref. 1) modified for partial feedforward.

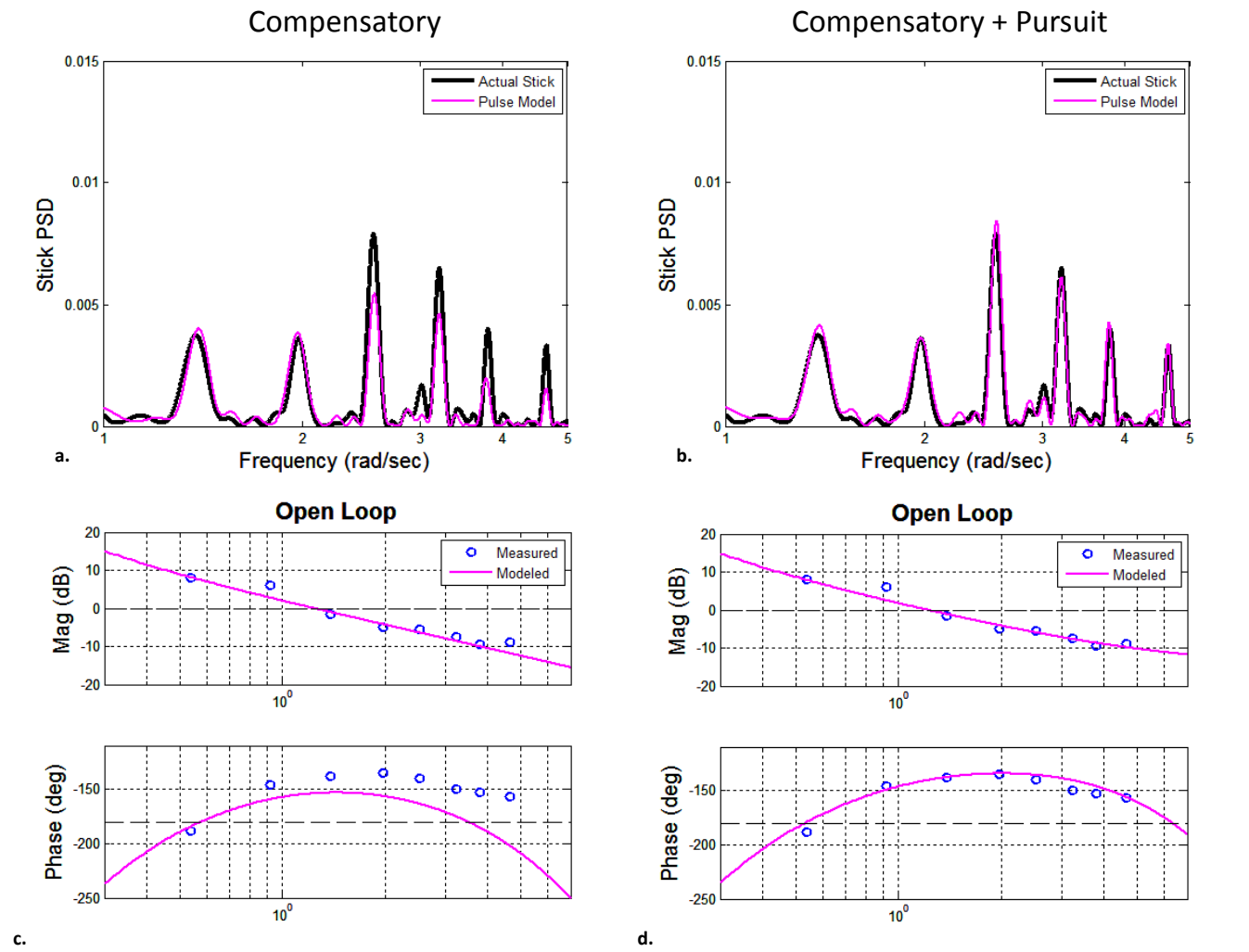

Figure 24. Effect of pursuit tracking: Power spectral density, a) Compensatory only; b) Pursuit with compensatory. Frequency response, c) Compensatory only; d) Pursuit with compensatory

CONCLUSIONS

The following summarize the conclusions of this paper:

1. A pilot model is proposed whose elements include the standard CM components (lead, time delay, and gain), perceptual noise, and a limiter that clips the CM output. A nonlinear pilot control technique, observed and coined by the authors as 'amplitude clipping', is shown to improve stability, performance, and reduce workload when employed with vehicle dynamics that require high lead compensation by the pilot. Combining linear and nonlinear methods a novel approach is used to measure the pilot control parameters when amplitude clipping is present, allowing precise measurement in real time of key pilot control parameters. It is hypothesized that it is easier for the pilot to clip amplitude (similar to bang-bang control) than to modulate the CM gain (without amplitude clipping) in response to changing internal and external variables.

2. Based on the results of an experiment designed to probe workload primary drivers, a method was developed that estimates pilot spare capacity (Bedford rating scale) from readily observable measures. From this experiment it appears that pilots attempt to minimize the error they control while using a minimum of control exertion – a combination of tracking and control economy. This relationship observed appears to be largely task-generic. To test reasonableness of the Bedford estimator it was applied to helicopter multi-axis flight. Given that the Bedford estimator was developed from a single-axis simulation task experiment, and that the DVE flight test conditions presented the pilots with multi-modal cueing (tactile, audio) and a mixed visual environment (head-down display and a distracting out-the-

window scene of actual blowing dust), the degree of correspondence between the actual and estimated pilot ratings is encouraging.

3. From the inflight test results it appears that during multi-axis operation (where each axis may affect the other's performance), the Bedford estimate for any given axis reflects the combined effects of all axes on that axis - and the individual estimates do not additively (even partially) contribute to the overall workload perception. The channel with the highest workload at any instant is responsible for the overall workload at that instant.

4. It was shown that the CM appears to drive a pilots' pulsing behavior in a very predictable manner. Roughly speaking, the pilot generates pulses such that the area under the pulse (pulse amplitude multiplied by pulse width) is approximately equal to area under the hypothetical CM output. This can allow a pilot to employ constant amplitude pulsing so that only the pulse duration (width) is modulated – a drastic simplification over the demands of continuous tracking.

5. It appears pursuit tracking may be activated when pulse control is employed.

6. Pilot technique such as amplitude-clipping, pulsing, and continuous tracking can have a significant influence on workload and performance, and a pilot's ability to maintain satisfactory performance in the presence of sudden external and internal changes. This presents the potential for test, evaluation, and even fleet pilots to learn different control strategies and optimally match and apply them to different tasks and environments.

Author contact:
Edward Bachelder edward.n.bachelder@nasa.gov
Bimal Aponso bimal.l.aponso@nasa.gov
Martine Godfroy-Cooper martine.godfroy-1@nasa.gov

ACKNOWLEDGMENTS

This work was supported by cooperative agreement NNX16AJ91A between the U.S. Army Aviation Development Directorate and San Jose State University. This paper has been approved for public release: unlimited distribution.

REFERENCES

1. McRuer, D., Krendal, E., *Mathematical Models of Human Pilot Behavior*, AGARD-AG-188. (1974).
2. Bachelder, E., Aponso, B.: *Novel Estimation of Pilot Performance Characteristics*, AIAA Atmospheric Flight Mechanics Conference, AIAA SciTech Forum, (AIAA 2017-1640)
3. Tischler, M., Remple, R., "Aircraft and Rotorcraft System Identification", AIAA, 2006.
4. Roscoe, A. H., & Ellis, G. A. (1990). *A subjective rating scale assessing pilot workload in flight. A decade of practical use*. Royal Aerospace Establishment. Technical Report 90019. Farnborough. UK: Royal Aerospace Establishment.
5. Mitchell, D., Aponso, B.,"Reassessment and extensions of pilot ratings with new data", 17th Atmospheric Flight Mechanics, Portland,OR, 1990.
6. Graham, D., McRuer, D., *Analysis of Nonlinear Control Systems*, New York, Wiley, 1961.